

Modeling and analysis of quadratic term in the wind effects on structures

A. Kareem^{a,*}, M.A. Tognarelli^a, K.R. Gurley^b

^a*NatHaz Modeling Laboratory, Department of Civil Engineering and Geological Sciences, University of Notre Dame, Notre Dame, IN 46556-0767, USA*

^b*Department of Civil Engineering, University of Florida, Gainesville, FL 32611, USA*

Abstract

Historically, the quadratic drag term containing the square of the fluctuating velocity component has been often ignored in analyses of wind-excited structures. This paper addresses a technique to model the contribution of this term to the system response extremes. Among the topics covered are the development of a non-Gaussian gust loading factor via moment-based Hermite transformation. A frequency domain analysis approach involving Volterra theory and higher-order response cumulant calculations from direct integrations or Kac-Siegert technique is employed to obtain information needed for this transformation. © 1998 Published by Elsevier Science Ltd. All rights reserved.

Keywords: Probabilistic wind modeling; Nonlinear analysis; Gust factor; Random vibration; Structural analysis; Extreme response; RMS response

1. Introduction

Several authors [1–8] have addressed the contribution of the quadratic drag force term to the mean-square response. These studies have acknowledged that for moderate levels of wind turbulence intensity this contribution is negligible. On the other hand, the importance of the quadratic term to response extremes has been shown to be much greater [9–13]. This paper presents a unified approach to assessing the importance of the quadratic drag term in terms of both mean-square system response (Eqs. (4) and (5)) and response extremes. The format of the discussion is the same as that found in building codes and standards in both the US and abroad.

* Corresponding author. E-mail: kareem@navier.ce.nd.edu.

The treatment of dynamic wind load effects in wind engineering is often facilitated by the introduction of a gust loading factor. Commonly used gust loading factors are based on linearization, i.e., they ignore the quadratic term in the expression of drag force. This paper will show a procedure in which the non-Gaussian character of the process is taken into account through moment-based Hermite transformation [12,14,15]. This transformation has been shown to represent more accurately the tail region of the PDF of a non-Gaussian process than the more commonly Edgeworth-series-based models. The present formulation reduces to standard Gaussian-based formulation for the case in which the quadratic term is neglected.

A Volterra system formulation is used to estimate the higher-order response cumulants of a nonlinear system exposed to wind loads. This frequency-domain framework includes the contribution of the quadratic term as well as the relative fluid-structure velocity which contributes aerodynamic damping to the system. The response skewness and kurtosis determined either via direct integration [12] or Kac–Siegert approach [16] become input to the moment-based Hermite transformation model for the gust factor. While analysis shows that the contribution of the quadratic term is not significant in terms of second-order statistics as alluded to earlier, its importance magnifies in the extreme response estimates. This trend is more noteworthy for relatively stiff structures. Notably, structures which are relatively more sensitive to background turbulence effects than the resonant portion of excitation are most affected by the inclusion of the quadratic term. In this regard, the inclusion of the squared term has definite design implication as most low- to mid-rise buildings are sensitive to only the background turbulence effects.

2. Modeling and analysis

2.1. Aerodynamic loading

The total wind force on a structure in the alongwind direction of the wind is given by

$$F(t) = \frac{1}{2}\rho AC_D(U + u - \dot{x})^2, \quad (1)$$

where ρ is the air density, A the projected area, C_D the alongwind force coefficient, U the mean wind speed and \dot{x} the structural speed. Different levels of approximation are made in using Eq. (1) for the analysis of wind-loaded structures. Typically, the quadratic terms introduced by u and \dot{x} are ignored. In this study, we wish to examine systematically the influence of various nonlinear terms on the wind loads and the associated structural response. First, analysis based on single point statistics is considered by ignoring the contribution of the feedback velocity term only:

$$F(t) = 1/2\rho AC_D U^2 + 1/2\rho C_D A U^2 \left[\frac{2u(t)}{U} + \frac{u^2(t)}{U^2} \right]. \quad (2)$$

The spectral description of the fluctuating portion of the wind force is given by

$$S_{F'}(f) = 4\gamma^2 U^2 S_u(f) + 2\gamma^2 \int_0^\infty S_u(f) S_u(f - f') df', \tag{3}$$

where prime denotes the fluctuating part and γ is equal to $\frac{1}{2}\rho AC_D$. By definition, the mean-square value of $F'(t)$ is given by

$$\overline{F'^2} = 4\gamma^2 U^2 \overline{u^2(t)} + 2\gamma^2 [\overline{u^2(t)}]^2 = \overline{F_1'^2} + \overline{F_2'^2}. \tag{4}$$

Normalizing Eq. (4) by $\overline{F_1'^2}$ and rearranging

$$(\overline{F'^2}/\overline{F_1'^2})^{1/2} = (1 + I^2/2)^{1/2} \tag{5}$$

in which $I = \sqrt{\overline{u^2}}/U$ is the turbulence intensity. The ratio between the RMS value of the quadratic term wind force to the linear term is given by $\sigma^{I21}/\sigma^{I1} = I/\sqrt{2}$. For a turbulence intensity of 15%, the quadratic term contribution is generally 10% of the linear force [5]. An example of a tension leg platform with an exposed area of 3376 m², drag coefficient of 1.2 and air density of 1 kg/m³ is given in Table 1 for three different spectra of wind fluctuations. The results show that the contribution of the quadratic term is indeed a function of the spectral description.

2.2. RMS response

The mean-square value of response is given by

$$\sigma_x^2 = \frac{4\sigma_u^2}{U^2} \overline{X^2} \int_0^\infty |H(i2\pi f)|^2 \chi^2(f) \left[S'_u(f) + \frac{I^2}{2} \Phi'_u(f) \right] df, \tag{6}$$

in which $|H(i2\pi f)|^2$ and $\chi^2(f)$ are the mechanical and aerodynamic transfer functions, respectively. The aerodynamic transfer function accounts for distortion of approach flow due to the presence of a structure and lack of correlation in the flow field. A simplified expression which has been found to be in satisfactory agreement with experimental observation is given by Ref. [17].

The preceding expression can be recast in the following form:

$$\sigma_x^2 = 4I^2 \overline{X^2} [A_B + A_R], \tag{7}$$

$$A_B = \int_0^\infty \chi^2(f) \left[S'_u(f) + \frac{I^2}{2} \Phi'_u(f) \right] df = B, \tag{8}$$

$$A_R = \chi^2(f_n) \left[S'_u(f_n) + \frac{I^2}{2} \Phi'_u(f_n) \right] \int_0^\infty |H(i2\pi f)|^2 df = \frac{SE}{\zeta_n}, \tag{9}$$

where $S = \chi^2(f_n)$, $E = \pi f_n [S'_u(f_n) + 0.5I^2 \Phi'_u(f_n)]/4$ and $S'_u(f)$ and $\Phi'_u(f)$ are obtained by normalizing $S_u(f)$ and $\Phi_u(f)$ with σ_u^2 and σ_u^4 , respectively. The above mathematical

Table 1

Mean, linear and quadratic wind force components on a TLP in surge

Spectrum	Mean wind velocity (m/s)	σ of fluctuation (m/s)	Mean wind force (kN)	$\sigma^{[1]}$ linear force (kN)	$\sigma^{[2]}$ quadratic force (kN)
Harris	29.6	3.39	1798.0	406.51	32.92
Davenport	29.6	3.22	1795.8	386.1	29.70
Kareem	29.6	3.81	1804.2	456.9	41.58

manipulation was carried out to recast this formulation in the format used by standards and specifications. B represents the background response contribution, S denotes the size reduction factor, E represents the gust energy factor and f_n and ξ_n are the natural frequency and damping, respectively, in the n th mode.

2.3. Peak response

The expected maximum value of random response X is given by

$$\bar{X}_{\max} = \bar{X} + g\sigma_x, \quad g = \sqrt{2 \ln vT} + 0.5772/\sqrt{2 \ln vT}, \quad (10)$$

where g is the peak factor for a Gaussian process [18] and v is the cyclic rate equal to $\sigma_x/(2\pi\sigma_x)$. In case the process under examination is non-Gaussian alternative means should be used to assess the peak factor. Refs. [9,12,13] have extended Davenport's Gaussian model to include non-Gaussian features. In these studies, it is noted that relatively stiff structures with higher damping values under high levels of turbulence exhibit maximum departure from Gaussianity. Kareem and associates evaluated the peak factor for the non-Gaussian case by employing the moment-based Hermite transformation which has been shown to be more accurate and robust in representing the tail regions of the PDF in a non-Gaussian process than the Edgeworth series employed in Ref. [9]. For the sake of brevity, only the final expression for the peak factor is reported here; details are given in Ref. [13],

$$g_{ng} = \kappa \left\{ \left(\beta + \frac{\gamma}{\beta} \right) + \hat{h}_3(\beta^2 + 2\lambda - 1) + \hat{h}_4 \left[\beta^3 + 3\beta(\gamma - 1) + \frac{3}{\beta} \left(\frac{\pi^2}{12} - \gamma + \frac{\gamma^2}{2} \right) \right] \right\} \quad (11)$$

where $\gamma = 0.5772$ (Euler's constant), $\beta = \sqrt{2 \ln v_{ng} T}$, κ , \hat{h}_3 , \hat{h}_4 are functions of skewness and kurtosis given by

$$v_{ng} = \frac{\sigma_x}{2\pi\sigma_x} (\kappa \sqrt{1 + 4\hat{h}_3^2 + 18\hat{h}_4^2})^{-1} \quad (12)$$

where $\hat{h}_3 = \gamma_3/(4 + 2\sqrt{1 + 1.5\gamma_4})$, $\hat{h}_4 = (\sqrt{1 + 1.5\gamma_4} - 1)/18$; $\kappa = (1 + 2\hat{h}_3^2 + 6\hat{h}_4^2)^{-1/2}$, γ_3 and γ_4 are skewness and kurtosis of x . For a Gaussian case, \hat{h}_3 , $\hat{h}_4 = 0$ and $\kappa = 1$ which reduces Eqs. (11) and (12) to the standard Gaussian forms given by Refs.

[14,18]. It should be noted that the expressions given for \hat{h}_3 and \hat{h}_4 above are approximations. In this study, an iterative approach is used to modify these coefficients so that the transformation better reflects the statistics of the process being analyzed.

Now the expected maximum value of response is given by

$$\begin{aligned} \bar{X}_{\max} &= \bar{X} + g_{ng} \left[2I \bar{X} \left(B + \frac{SE}{\xi_n} \right)^{1/2} \right], \\ G_{ng} &= \frac{\bar{X}_{\max}}{\bar{X}} = 1 + g_{ng} \left[2I \left(B + \frac{SE}{\xi_n} \right)^{1/2} \right]. \end{aligned} \tag{13}$$

Eq. (13) describes a non-Gaussian gust factor that includes contribution of the u^2 term. This expression reduces to classical expression if the u^2 term is dropped.

2.4. Computation of cumulants

In this section, a Volterra series and Kac–Seigert based approaches are used to compute higher-order cumulants necessary for the moment-based Hermite transformation. Only a brief description of each is given, details can be found in Ref. [12].

2.5. Volterra series approach

Mathematically, the velocity squared term in Eq. (1) can be expanded and approximately truncated as the following:

$$\begin{aligned} (u + U - \dot{x})^2 &= (u + U - \dot{x}_1)^2 - 2(u + U - \dot{x}_1)\dot{x}_2 + \dot{x}_2^2 \\ &\cong (u + U - \dot{x}_1)^2 - 2b\dot{x}_2, \end{aligned} \tag{14}$$

where $b = E[u + U - \dot{x}_1] = U$, and \dot{x}_1 and \dot{x}_2 represent linear and nonlinear components of response. While this general expansion includes the effects of fluid-structure interaction by including the structural velocity in the drag force expression, it may also be used when this effect is neglected. Note that the first term in Eq. (14) represents the square of a Gaussian process, while the second term represents the additional damping of the second-order dynamic system. Now, the equation of structural motion can be expressed as a system

$$M\ddot{x}_1 + (C + a_1)\dot{x}_1 + Kx_1 = a_1u, \quad M\ddot{x}_2 + (C + a_1)\dot{x}_2 + Kx_2 = (a_2/2)(u - \dot{x}_1)^2, \tag{15}$$

where $a_1 = \rho C_D A U$ and $a_2 = \rho C_D A$ [12]. Both systems have the transfer function,

$$H(\omega) = [K - \omega^2 M + i\omega(C + a_1)]^{-1}. \tag{16}$$

The input of the second-order system can be viewed as the output of $u(t)$ through a linear filter, with the transfer function, $H_v(\omega) = 1 - a_1 i\omega H(\omega)$. Then, the second-order transfer function, related to $u(t)$, is given by

$$H_2(\omega_1, \omega_2) = H(\omega_1 + \omega_2)H_v(\omega_1)H_v(\omega_2). \tag{17}$$

The expressions for the cumulants and power spectrum for the foregoing systems are given in the following. For the sake of brevity, let $H(1)$, $H(1 + 2)$, and $D(1)$ represent $H(\omega_1)$, $H(\omega_1 + \omega_2)$, and $D(\omega_1)d\omega_1$, respectively,

$$\begin{aligned}
 k_1 &= \frac{a_2^2 \sigma_u^2}{2} H(0), & k_2 &= a_1^2 \sigma^2 + \frac{a_2^2}{2} \int_{-\infty}^{\infty} \int_{-\infty}^{\infty} |H(1 + 2)|^2 H_v(1) H_v(2) |D(1) D(2)|, \\
 k_3 &= 3a_1^2 a_2 \int_{-\infty}^{\infty} \int_{-\infty}^{\infty} H(1) H(2) H(-1 - 2) H_v(-1) H_v(-2) D(1) D(2) \\
 &\quad + a_2^3 \int_{-\infty}^{\infty} \int_{-\infty}^{\infty} H(1 + 2) H(-1 + 3) H(-2 - 3) |H_v(1) H_v(2) H_v(3)|^2 D(1) D(2) D(3) \\
 k_4 &= 12a_1^2 a_2^2 \int_{-\infty}^{\infty} \int_{-\infty}^{\infty} H(1) H(2) H(-1 + 3) H(-2 - 3) H_v(-1) H_v(-2) \\
 &\quad \times |H_v(-3)|^2 D(1) D(2) D(3) \\
 &\quad + 3a_2^4 \int_{-\infty}^{\infty} \int_{-\infty}^{\infty} H(1 + 2) H(-1 + 3) H(-2 + 4) H(-3 - 4) \\
 &\quad \times |H_v(1) H_v(1) H_v(3) H_v(4)|^2 D(1) D(2) D(3) D(4). \tag{18}
 \end{aligned}$$

The evaluation of the fourth-order cumulant was considered computationally prohibitive previously, not only because of the nature of the integrand, but also because of the extensive computational effort needed to determine the multi-fold integrals [19]. In Ref. [12], the preceding integrals have been rearranged to facilitate computational efficiency. Details are omitted here for the sake of brevity.

2.6. Kac–Siegert approach

There is an alternative approach to obtain the higher-order cumulants by Kac–Siegert technique [16]. Each component of the response is cast as an eigenfunction expansion. When the second-order response kernel, $Q_2(x, y)$, is Hermitian, the orthogonal eigenfunctions, $\phi_i(\cdot)$, are determined as the characteristic functions of the following Fredholm homogeneous integral equation of second kind:

$$\int_a^b Q_2(x, y) \phi(y) dy = \lambda \phi(x). \tag{19}$$

The nontrivial characteristic values of Eq. (19) are real, and the corresponding characteristic functions are orthogonal to each other. Due to the orthogonality,

simplification yields

$$Q_2(x, y) = \sum_{i=1}^{\infty} \lambda_i \phi_i(x) \phi_i^*(y). \tag{20}$$

Presently, the kernel is given as

$$Q_2(x, y) = G(x)H_{\nu}(x)H(x - y)H_{\nu}(-y)G(y), \tag{21}$$

where $G(x) = [D(x)]^{1/2}$, and $Q_2(x, y)$ are Hermitian and both x and y represent frequency. The foregoing equations can be solved numerically to obtain the eigenvalues and corresponding eigenvectors. Accordingly, the cumulant expressions for the system (Eq. (15)) are given as

$$k_n = \sum_{i=1}^M \left[\frac{n!}{2} (a_1 \alpha_i)^2 (a_2 \lambda_i)^{n-2} (1 - \delta_{n1}) + \frac{(n-1)!}{2} (a_2 \lambda_i)^n \right], \tag{22}$$

where α_i are coefficients of the eigenfunction expansion of the first-order response and M is the number of terms retained. The third- and fourth-order cumulants are significant and have physical meanings related to skewness and kurtosis. In particular, for the moment-based Hermite transformation, $\gamma_3 = k_3/k_2^{3/2}$ and $\gamma_4 = k_4/k_2^2$.

3. Examples

Table 2 illustrates a comparison of the peak factor of the response of the SDOF water tower given in Ref. [11]. The peak factors computed via the present moment-based Hermite transformation method compare well with the results of that study and reaffirm the shortcomings of an earlier non-Gaussian estimation method as well as the Gaussian approximation (quadratic term in drag force neglected) to the peak factor.

Table 2
Comparison of peak factors

Case	Ref. wind (m/s)	Power law exponent	RMS (m/s)	ζ (%)	g (Gaussian)	g_{ng}		
						Soize [9]	Grigoriu [11]	Present study
<i>h</i> = 20 m, <i>M</i> = 2161 kg, <i>K</i> = 85 300 N/m								
1	28	0.15	4.6	5	4.04	4.64	5.18	5.09
2	13	0.35	5.8	3	4.10	4.91	6.43	6.50
3	13	0.35	5.8	5	4.04	4.86	6.42	6.44
<i>h</i> = 80 m, <i>M</i> = 13 500 kg, <i>K</i> = 85 300 N/m								
4	28	0.15	4.6	3	3.87	4.29	4.59	4.49
5	28	0.15	4.6	5	3.85	4.31	4.63	4.56
6	13	0.35	5.8	3	3.87	4.43	5.13	5.01
7	13	0.35	5.8	5	3.85	4.45	5.12	5.14

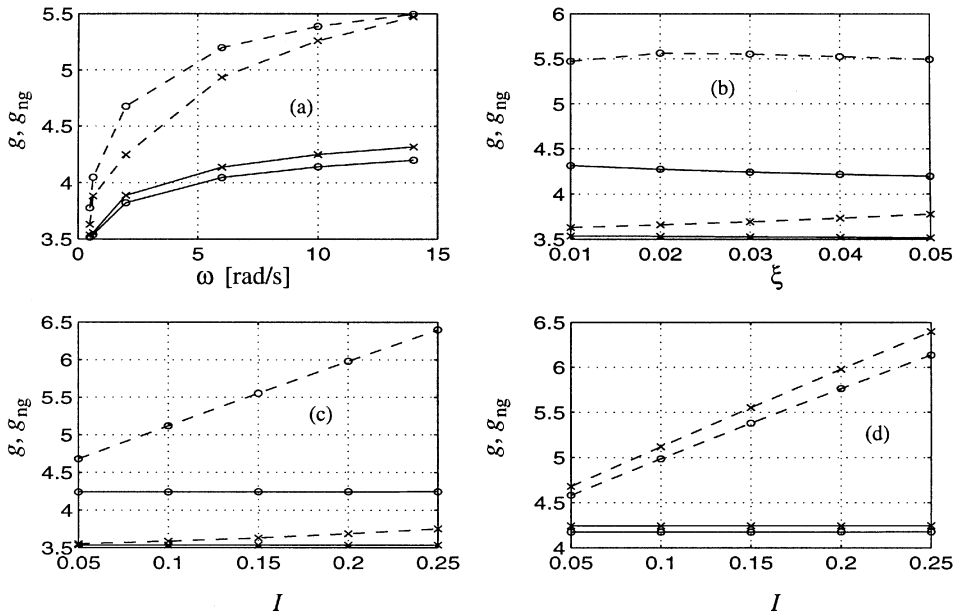


Fig. 1. Solid Gaussian; dashed, non-Gaussian, (a) \times , $\zeta = 0.01$, $I = 0.15$; \circ , $\zeta = 0.05$, $I = 0.15$; (b) \times , $\omega = 0.5$, $I = 0.15$; \circ , $\omega = 14$, $I = 0.15$; (c) \times , $\omega = 0.5$, $\zeta = 0.01$; \circ , $\omega = 14$, $\zeta = 0.03$; (d) $\omega = 14$, $\zeta = 0.03$ \times , Harris spectrum; \circ , Blunt spectrum [11].

The sensitivity of the peak factor to structural frequency, turbulence intensity, damping ratio, and input spectrum is illustrated through an example single degree of freedom floating offshore structure subjected to wind drag loads. The random wind field is modeled in these examples by the Harris wind spectrum and the mean wind velocity is 20 m/s. The results are for drag solely as a function of wind velocity, the influence of the structural velocity in this particular example is negligible. In Fig. 1a, the variation in the peak factor over a wide range of structural natural frequencies, ω , is shown for both Gaussian and non-Gaussian peak factors assuming low and high damping. The peak factor almost doubles over the range of natural frequency (structural stiffness). Fig. 1b indicates that changes in damping values, ζ , have a much less significant effect on the peak factor. Fig. 1c shows that the effect of turbulence intensity, I , is most pronounced for stiffer structures with higher damping. Fig. 1d illustrates that similar trends are exhibited by the peak factor over a range of turbulence intensities when the wind field is modeled by the Harris spectrum or the blunt spectrum given in Ref. [11]. All of these figures indicate that the Gaussian approximation leads to non-conservative estimates of the peak factor.

Underestimation of the gust factor by ignoring the u^2 term in the drag force is shown in Fig. 2. This figure shows that the Gaussian approximation leads to non-conservative estimates of the gust factor, G , as well. Fig. 2a and 2b illustrate that the gust factor decreases as the structural stiffness and damping ratio increase. Further,

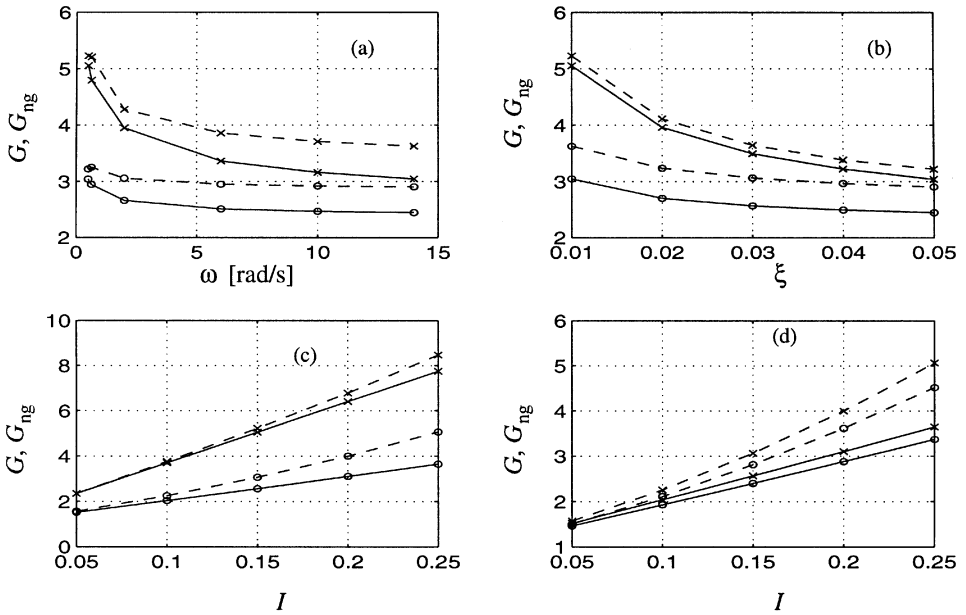


Fig. 2. Solid Gaussian; dashed, non-Gaussian, (a) \times , $\zeta = 0.01$, $I = 0.15$; \circ , $\zeta = 0.05$, $I = 0.15$; (b) \times , $\omega = 0.5$, $I = 0.15$; \circ , $\omega = 14$, $I = 0.15$; (c) \times , $\omega = 0.5$, $\zeta = 0.01$; \circ , $\omega = 14$, $\zeta = 0.03$; (d) $\omega = 14$, $\zeta = 0.03$ \times , Harris spectrum; \circ , Blunt spectrum [11].

these figures indicate that the increase in the gust factor introduced by non-Gaussianity is most pronounced for stiffer structures. Fig. 2c shows that the gust factor increases with increasing turbulence intensity, again, with a greater impact of non-Gaussianity on the stiffer structure. Finally, Fig. 2d shows that for the two wind field spectral models chosen for comparison, the behavior of the gust factors for increasing turbulence intensity and due to non-Gaussianity is very similar.

4. Concluding remarks

A unified treatment of the effect of the quadratic velocity term in the wind force on structures has been presented. The discussion has covered not only the mean-square response, but also the extremes of the response and has been cast in a framework common to building codes and standards. The quantification of the expected extreme response has been further facilitated by the introduction of a non-Gaussian peak factor which employs the system response cumulants in a moment-based Hermite transformation PDF model. In general, the inclusion of the quadratic velocity term increases both the mean-square and the expected extreme response of a system, having a more significant impact upon the latter. Furthermore, a parameter study indicates

that the increase in the expected extreme response is more pronounced for structures which are stiffer and hence more susceptible to background turbulence.

Acknowledgements

The support for this research was provided in part by the Office of Naval Research Grant N00014-93-1-0761 and the National Science Foundation Grant CMS 95-03779.

References

- [1] R.I. Harris, The response of structures to gusts, *Wind Effects Bldgs. Struct.*, HMSO, London, I (1965) pp. 394–421.
- [2] C. Floris, Equivalent gaussian process in stochastic dynamics with application to along-wind response of structures, *Int. J. Non-linear Mech.* 31 (1996) 779–794.
- [3] A. Kareem, Wind excited motion of buildings, Ph.D. Dissertation, Dept. of Civ. Eng., Colorado State Univ, 1978.
- [4] K. Gurley, A. Kareem, Gust loading factors for tension leg platforms, *Appl. Ocean Res.* 15 (1993) 137–154.
- [5] A. Kareem, Nonlinear wind velocity term and response of compliant offshore structures, *J. Eng. Mech. ASCE* 110 (1984) 1573–1588.
- [6] R. Vaicaitis, E. Simiu, Nonlinear pressure terms and alongwind response, *J. Struct. Div. ASCE* 103 (1977) 903–906.
- [7] A. Kareem, Y. Li, Stochastic response of a tension leg platform to wind and wave fields, Tech. Rpt. No. UHCE 88-18, Dept. of Civ. Eng., Univ. of Houston, 1988.
- [8] V. Kolousek, M. Pirner, O. Fischer, J. Naprstek, *Wind Effects on Civil Engineering Structures*, Elsevier, Amsterdam, 1984.
- [9] C. Soize, Gust loading factors with nonlinear pressure terms, *J. Struct. Div. ASCE* 104 (1978) 991–1007.
- [10] S. Benfratello, G. Falsone, G. Muscolino, Influence of the quadratic term in the alongwind stochastic response of SDOF structures, *Eng. Struct.* 18 (1966) 685–695.
- [11] M. Grigoriu, Response of linear systems to quadratic gaussian excitations, *J. Eng. Mech. ASCE* 112 (1986) 523–535.
- [12] A. Kareem, J. Zhao, Analysis of non-gaussian surge response of tension leg platforms under wind loads, *J. Offshore Mech. Arctic Eng. ASME* 116 (1994) 137–144.
- [13] K.R. Gurley, M.A. Tognarelli, A. Kareem, Analysis and simulation tools for wind engineering, *Prob. Engrg. Mech.* 12 (1997) 9–31.
- [14] M. Grigoriu, Crossing of non-gaussian translation process, *J. Eng. Mech. ASCE* 110 (1984) 610–620.
- [15] S.R. Winterstein, Non-normal responses and fatigue damage, *J. Eng. Mech. ASCE* 111 (1985) 1291–1295.
- [16] M. Kac, A. Siebert, On the theory of noise in radio receivers with square law detectors, *J. Appl. Phys.* 8 (1947) 383–397.
- [17] B.J. Vickery, On the reliability of gust loading factors, U.S. Dept. of Commerce, Nat'l. Bureau of Standards Bldg. Sci. Series 30, 1969.
- [18] A.G. Davenport, Note on the distribution of the largest value of a random function with application to gust loading, *Proc. of the Instit. of Civ. Engrs. London* 28 (1964) 187–196.
- [19] E. Bedrosian, S. Rice, The output properties of volterra systems (nonlinear systems with memory) driven by harmonic and gaussian inputs, *Proc. IEEE* 59 (1971) 1688–1707.